




Subharmonic spin correlations and spectral pairing in Floquet time crystalsAlexander-Georg Penner,¹ Harald Schmid ¹, Leonid I. Glazman ², and Felix von Oppen ¹¹*Dahlem Center for Complex Quantum Systems and Fachbereich Physik, Freie Universität Berlin, 14195 Berlin, Germany*²*Department of Physics and Yale Quantum Institute, Yale University, New Haven, Connecticut 06520, USA*

(Received 23 February 2025; accepted 26 April 2025; published 8 May 2025)

Floquet time crystals are characterized by the subharmonic behavior of temporal correlation functions. Studying the paradigmatic time crystal based on the disordered Floquet quantum Ising model, we show that its temporal spin correlations are directly related to spectral characteristics and that this relation provides analytical expressions for the correlation function of finite chains, which compare favorably with numerical simulations. Specifically, we show that the disorder-averaged temporal spin correlations are proportional to the Fourier transform of the splitting distribution of the pairs of eigenvalues of the Floquet operator, which differ by π to exponential accuracy in the chain length. We find that the splittings are well described by a log-normal distribution, implying that the temporal spin correlations are characterized by two parameters. We discuss possible implications for the phase diagram of Floquet time crystals.

DOI: [10.1103/PhysRevB.111.184308](https://doi.org/10.1103/PhysRevB.111.184308)**I. INTRODUCTION**

There has recently been much interest in the possibility of spontaneous breaking of time translation symmetry [1–10]. While spontaneous breaking of spatial translation symmetries underlies equilibrium crystalline phases, time translation symmetry breaking has been established only under out-of-equilibrium conditions. This has led to the concept of Floquet time crystals, with the Floquet quantum Ising chain providing a paradigmatic model [11,12]. Randomness in the exchange couplings as well as in integrability-breaking fields introduces localization, which suppresses thermalization and enables subharmonic temporal spin correlations.

The subharmonic correlations are closely related to spectral properties of the Floquet operator. In the case of the Floquet quantum Ising model, its eigenstates appear in pairs with eigenphases that differ by π (taking the period of the Floquet drive to be equal to $T = 1$). While this pairing becomes exact in the thermodynamic limit, there are deviations from π for finite chains. As discussed in Refs. [13,14], the typical deviations are exponentially small in the system size. Here, we show that the probability distribution of these splittings away from π is accurately described by a log-normal distribution. Moreover, the disorder-averaged temporal spin correlation function of the time crystal is directly proportional to the Fourier transform of the splitting distribution, providing an analytical description of the temporal spin correlations and their evolution with the chain length.

Earlier studies of the spectral diagnostics of Floquet time crystals focused on the statistics of adjacent energy levels and

measures of entanglement [11,15–20]. While thermalizing systems tend to follow Wigner-Dyson-like level repulsion, the absence of level repulsion is closely related to obstructions to thermalization. Unlike these more generic measures of spectral correlations, the distribution of π pairings is directly related to the defining temporal spin correlations of discrete time crystals. The deviations Δ from perfect π pairing lead to a decay of the subharmonic spin correlations at times which are exponentially long in the system size. Our results show that the distribution of π pairings directly controls how the time-crystalline state is established in the thermodynamic limit. Moreover, the log-normal distribution of Δ entails that temporal spin correlations of finite-size systems are characterized by two parameters, namely, the average and the variance of $\ln \Delta$.

Our results are based on a combination of numerical simulations and analytical arguments for a disordered Floquet quantum Ising chain, both without and with longitudinal random field. The appearance of a log-normal distribution can be traced to the fact that the deviations from π pairings are related to tunneling processes traversing the entire Floquet quantum Ising chain. The two partner states are even and odd eigenstates of the spin-flip symmetry of the Ising model. In the limit of weak transverse fields, their splitting reflects tunneling processes between two oppositely polarized eigenstates of the ferromagnet. Effectively, this occurs by propagation of a domain wall around the system, and the associated amplitude is a product of a large number of random factors.

Alternatively, this can be viewed from the fermionized version of the model [21,22]. In this formulation, the two partner states have opposite fermion parities. The sectors with even and odd fermion parities (known as the Neveu-Schwarz and Ramond sectors) satisfy antiperiodic and periodic boundary conditions of the Jordan-Wigner fermions, respectively. Consequently, the splittings reflect the sensitivity to boundary conditions. In localized systems, the sensitivity to boundary

Published by the American Physical Society under the terms of the Creative Commons Attribution 4.0 International license. Further distribution of this work must maintain attribution to the author(s) and the published article's title, journal citation, and DOI.

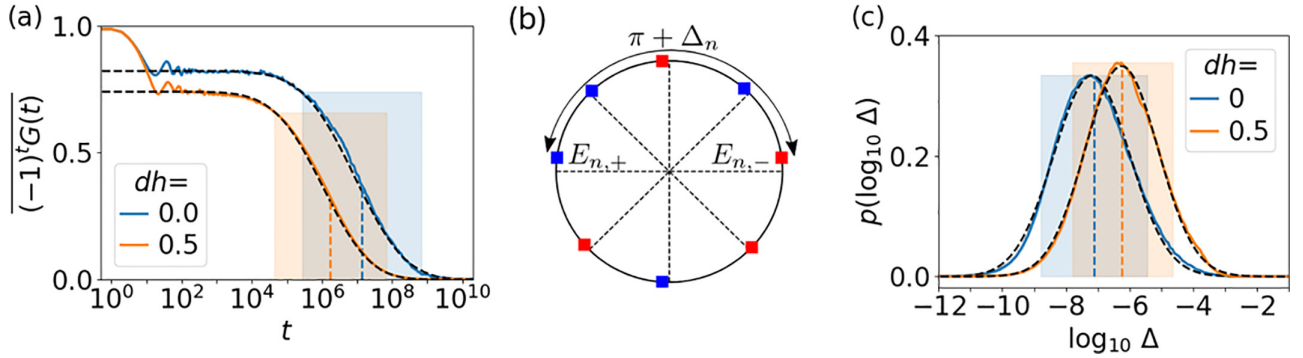


FIG. 1. (a) Disorder average of the bulk spin correlation function $G(t)$ (solid lines) of a discrete time crystal without (blue) and with (orange) longitudinal fields. Dashed lines: Fourier transform $p(t)$ of a log-normal distribution $p(\Delta)$ with cumulants extracted from the splitting distribution. $p(t)$ was multiplied by an overall prefactor to match the plateau value of $G(t)$. Decay range (shaded boxes) and location (vertical dashed lines) are estimated from $p(\log_{10} \Delta)$ in (c), with corresponding labeling. (b) Illustration of the many-body Floquet spectrum with π -paired partner states. Even and odd states under the spin-flip symmetry are indicated by blue and red squares. The sketch also indicates the finite-size splittings Δ_n away from π . (c) Numerical splitting distributions (solid lines) without (blue) and with (orange) longitudinal fields, compared to log-normal fits (dashed lines). The splitting distribution is sampled across the many-body spectrum and disorder ensemble. Shaded boxes: characteristic range determining the timescales of spin correlations in (a); see the text for further discussion. Parameters are $N = 12$, $g = 0.95$, $dJ = 0.25$, $J = 0.5$, and $\mathcal{N} = 10^3$ disorder realizations.

conditions is frequently characterized by log-normal distributions, as for the conductance [23], the level curvatures [24], and the splitting of end states [25].

The remainder of this paper is structured as follows. In Sec. II, we use numerical simulations to establish a relation between the temporal spin correlations of the Floquet time crystal and the splitting distribution of the π pairs. Section III supports our numerical results with analytical considerations. In particular, we analyze the splitting distribution within the original spin model in Sec. III A and within the framework of Jordan-Wigner fermions in Sec. III B. The effects of an integrability-breaking longitudinal field are discussed in the framework of a self-consistent perturbation theory in Sec. III C. We conclude in Sec. IV.

II. TEMPORAL SPIN CORRELATIONS AND SPECTRAL PAIRING: NUMERICAL RESULTS

We study the Floquet quantum Ising chain with random exchange couplings and random longitudinal field as a model for discrete time crystals. The Floquet operator

$$U_F = e^{\frac{ig}{2} \sum_{j=1}^N X_j} e^{\frac{ij}{2} \sum_{j=1}^N J_j Z_j Z_{j+1}} e^{\frac{ih}{2} \sum_{j=1}^N h_j Z_j} \quad (1)$$

defines the stroboscopic time evolution $|\Psi(t)\rangle = U_F^t |\Psi(0)\rangle$ of an initial state $|\Psi(0)\rangle$ after $t = 0, 1, 2, \dots$ cycles. Here, X_j and Z_j are Pauli operators at site j , and we assume periodic boundary conditions, i.e., $Z_{N+1} = Z_1$. We draw the Ising couplings J_j and longitudinal fields h_j from independent box distributions, $J_j \in [J - dJ, J + dJ]$ and $h_j \in [-dh, dh]$. The Floquet operator can be diagonalized, $U_F |n\rangle = e^{-iE_n} |n\rangle$, with E_n being eigenphases and $|n\rangle$ being Floquet eigenstates. The eigenphases can be restricted to the first Floquet zone, $-\pi \leq E_n \leq \pi$. The quantum Ising model ($dh = 0$) has a spin-flip symmetry, $P = \prod_j X_j$, and is integrable. The random longitudinal field breaks integrability. Spin-flip symmetry is broken for particular realizations of the longitudinal field but is maintained, on average, by the disorder ensemble.

Time-crystalline behavior occurs for transverse fields g close to 1 [11,12]. We characterize the dynamics of the time crystal by the infinite-temperature correlation function

$$G_j(t) = \langle Z_j(t) Z_j(0) \rangle, \quad (2)$$

where $Z_j(t) = (U_F^\dagger)^t Z_j (U_F)^t$ and $\langle \dots \rangle = 2^{-N} \text{tr}[\dots]$ averages over a complete set of states. We focus on the disorder-averaged correlation function $\overline{(-1)^t G(t)}$ (as denoted by the overline). The disorder average makes the correlation function translationally invariant for periodic boundary conditions, so we drop the site index j . At $g = 1$ and $dh = 0$, the transverse field flips all spins periodically, resulting in perfect period doubling, as diagnosed by $G(t) = (-1)^t$. Away from $g = 1$, the transverse field no longer induces complete spin flips. Provided that g does not deviate too far from $g = 1$, one finds that following initial transients, $(-1)^t G(t)$ plateaus for many cycles before slowly decaying to zero at very long times. This characteristic behavior remains qualitatively unchanged in the presence of the random longitudinal field. Figure 1(a) shows corresponding numerical results both without and with random longitudinal field.

The period-doubling characteristic of discrete time crystals originates from a spectrum-wide pairing of eigenstates [Fig. 1(b)]. For $dh = 0$, the partner states $|n, \pm\rangle$ are even (+) and odd (-) under the spin-flip symmetry P and have eigenphases $E_{n,\pm}$ differing by π up to finite-size corrections, which are exponentially small in the length N of the chain. The operators Z_j are odd under the spin-flip symmetry and couple partner states, resulting in the period doubling of $G(t)$. This follows from writing Eq. (2) in terms of exact eigenstates,

$$G_j(t) = \frac{1}{2^N} \sum_{nm} |\langle n | Z_j | m \rangle|^2 e^{i(E_n - E_m)t}. \quad (3)$$

This equation also implies that provided they are inhomogeneous across the spectrum, the finite-size deviations from π pairing cause the time-crystal oscillations to decay at exponentially long times.

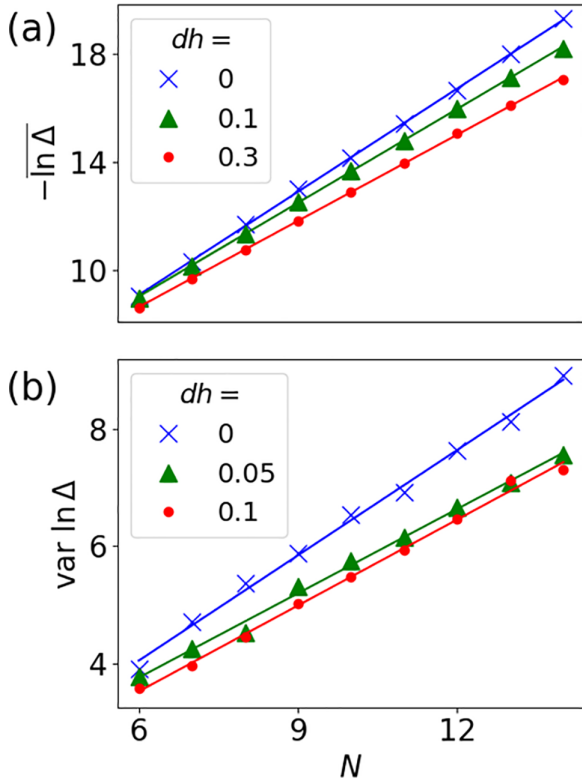


FIG. 2. Dependence on chain length N of the (a) mean and (b) variance of many-particle splittings, both without and with random longitudinal field (see legends). Averages and variances are extracted from log-normal fits to the entire splitting distribution. Symbols: data; solid lines: linear fits. Parameters are $J = 0.5$, $dJ = 0.25$, and $g = 0.95$. Disorder averages are over $\mathcal{N} = 5 \times 10^3$ realizations ($dh > 0$, $N = 6, \dots, 13$), $\mathcal{N} = 2 \times 10^3$ realizations ($dh > 0$, $N = 14$), and $\mathcal{N} = 2 \times 10^4$ realizations ($dh = 0$, all N).

To probe the relation between spectral pairing and time-crystal oscillations more closely, we compute the deviations $\Delta_n = \pi - E_{n,+} + E_{n,-}$ of the splittings from π across the Floquet spectrum and the disorder ensemble by exact diagonalization. Since paired eigenphases are almost antipodal, they can be identified by sorting the spectrum provided that the splittings are small compared to the level spacing. We show below that this condition is satisfied for transverse fields, which are sufficiently close to $g = 1$ [see Eq. (8)]. We characterize the splittings by their distribution function across the many-body spectrum and the disorder ensemble, which is shown in Fig. 1(c) both without and with longitudinal field. We find that in both cases, the splitting distribution is well fit by a log-normal distribution,

$$p(\ln \Delta) d \ln \Delta = \frac{1}{\sqrt{2\pi\sigma}} e^{-\frac{1}{2\sigma^2}(\ln \Delta - \mu)^2} d \ln \Delta. \quad (4)$$

Small deviations from the log-normal distribution appear in the tails of the distribution and are more pronounced without random longitudinal field.

The log-normal distribution is fully determined by the first two cumulants of $\ln \Delta$. Figure 2 shows the scaling of these

cumulants with system size N . We read off that

$$\mu = \overline{\ln \Delta} = -\frac{N}{\zeta}, \quad \sigma^2 = \text{var} \ln \Delta = \frac{N}{\lambda}. \quad (5)$$

The average $\overline{\ln \Delta}$ (characterizing typical values of Δ) decreases linearly in the chain length N . In contrast, the variance $\text{var} \ln \Delta$ grows with N . The prefactors of N define characteristic lengths ζ and λ , respectively. Figure 1(c) shows that as a function of the random longitudinal field, the average increases (the shift to the right), while the variance shrinks (the reduced width and increased peak height).

It is our central result that beyond initial transients, the Fourier transform

$$p(t) = \int d\Delta p(\Delta) e^{i\Delta t} \quad (6)$$

of the log-normal splitting distribution closely tracks the correlation function $\overline{(-1)^j G(t)}$. Figure 1(a) shows that $p(t)$ (dashed lines) matches $\overline{(-1)^j G(t)}$ (solid lines) up to an overall prefactor. This can be understood based on Eq. (2). The period-2 oscillations arise from the contributions of the π -paired levels. If fluctuations of the positive matrix-element prefactor across the spectrum or the disorder ensemble do not affect the temporal spin correlations, Eq. (2) yields

$$\overline{(-1)^j G(t)} \simeq \frac{A}{2^{N-1}} \text{Re} \sum_n \overline{e^{i(\pi - E_{n,+} + E_{n,-})t}}, \quad (7)$$

with the prefactor well approximated by

$$A \simeq \frac{1}{2^{N-1}} \sum_n \overline{|\langle n, + | Z_j | n, - \rangle|^2}.$$

This relates the temporal spin correlations to the Fourier transform of the splitting distribution.

The relation between Eq. (6) and the temporal spin correlations implies that the latter are controlled by the two cumulants, μ and σ , of the log-normal distribution. In particular, we can express the two characteristic times of the spin correlation function in terms of these cumulants. The bulk of the log-normal distribution falls into the range $\mu - \sqrt{2}\sigma \lesssim \ln \Delta \lesssim \mu + \sqrt{2}\sigma$. Correspondingly, its Fourier transform remains constant for $t \lesssim t^* = \exp(-\mu - \sqrt{2}\sigma)$ and falls off over the interval between t^* and $t^{**} = \exp(-\mu + \sqrt{2}\sigma)$, as illustrated by the shaded boxes in Figs. 1(a) and 1(c). In combination with Eq. (5) this implies that time-crystalline behavior, i.e., a nonzero $\overline{G(t)}$, persists for all times when taking the thermodynamic limit before the $t \rightarrow \infty$ limit. We can also check that the ratio between “maximal” splitting $\exp(\mu + \sqrt{2}\sigma)$ and many-body level spacing $\propto 2^{-N}$ vanishes for $N \rightarrow \infty$ as long as

$$\zeta < 1/\ln 2, \quad (8)$$

i.e., as long as g is sufficiently close to unity, as mentioned above, ensuring that the splitting distribution is well-defined.

An approximate analytical expression for $p(t)$ can be obtained by evaluating the Fourier transform over the log-normal distribution within the saddle-point approximation. Keeping

only quadratic deviations from the saddle, one finds [26]

$$p(t) \simeq \text{Re} \frac{\exp \left\{ -\frac{1}{2\sigma^2} [W^2(-i\sigma^2 e^{\mu t}) + 2W(-i\sigma^2 e^{\mu t})] \right\}}{\sqrt{1 + W(-i\sigma^2 e^{\mu t})}}, \quad (9)$$

where W is the Lambert- W function defined by $W(x)e^{W(x)} = x$. Equation (9) is controlled in the limit of small σ but reproduces the Fourier transform qualitatively even when σ is of order unity. One also deduces the approximate expression $p(t) \simeq e^{-(1/(2\sigma^2)) \ln^2(\sigma^2 e^{\mu t})}$ for the asymptote at large t .

III. ANALYTICAL CONSIDERATIONS

A. Spin model

We explore the spectral properties underlying these numerical results by analytical considerations in limiting cases. We first focus on the Floquet operator $U_{F,0} = U_F(h_j = 0)$ in the absence of the random longitudinal field h_j ,

$$U_{F,0} = P e^{\frac{i\pi\delta g}{2} \sum_{j=1}^N X_j} e^{\frac{i\pi}{2} \sum_{j=1}^N J_j Z_j Z_{j+1}}. \quad (10)$$

Since we are interested in Floquet operators with transverse field g close to 1, we have pulled out an overall factor of $P = \prod_j X_j$ by writing $g = 1 + \delta g$, with $\delta g \ll 1$. The Floquet evolution commutes with the spin-flip symmetry, so we can consider the even ($P = 1$) and odd ($P = -1$) sectors of the model separately. In the limit of $\delta g \rightarrow 0$, the eigenstates of $U_{F,0}$ for $P = \pm 1$ are even and odd linear combinations of oppositely polarized bit strings, e.g.,

$$\frac{1}{\sqrt{2}} (|\uparrow\downarrow\downarrow\cdots\downarrow\rangle \pm |\downarrow\uparrow\uparrow\cdots\uparrow\rangle). \quad (11)$$

Due to the overall factor of P , the corresponding eigenvalues are $\pm e^{iE}$, with E and $E + \pi$ being antipodal eigenphases.

Splittings away from π appear for nonzero δg . We consider the regime of intermediate disorder strength,

$$\delta g \ll dJ \ll J \ll 1. \quad (12)$$

This allows us to approximate the Floquet operator as

$$U_{F,0} \simeq P e^{\frac{i\pi\delta g}{2} \sum_{j=1}^N X_j + \frac{i\pi}{2} \sum_{j=1}^N J_j Z_j Z_{j+1}}, \quad (13)$$

where the exponent is the Hamiltonian of the transverse field Ising model with a small transverse field. Thus, the splittings can be obtained from ordinary Hamiltonian perturbation theory in δg .

The splittings arise from tunneling between the two oppositely polarized bit strings in Eq. (11) induced by spin flips of amplitude δg . Since J is largest, all exchange couplings are positive, and to leading order, the number of domain walls remains unchanged in the virtual intermediate states. Considering a state with two domain walls (the smallest number compatible with periodic boundary conditions) for definiteness, a tunneling event can be thought of as a process in which the two domain walls trade locations in such a way that the N hops effectively make a full loop around the system. The corresponding splitting appears in N th-order perturbation theory with amplitude

$$\Delta_{I,K} \simeq \frac{\pi\delta g}{2} \sum_{\gamma} \prod_{(i,j) \in \gamma} \frac{\delta g}{J_i + J_K - J_i - J_j}, \quad (14)$$

where I and K denote the locations of the domain walls of the π pair. The sum is over all contributing trajectories γ , with (i, j) running through the $N - 1$ intermediate configurations with domain walls located at i and j .

A log-normal splitting distribution is a plausible consequence of the appearance of products with an extensive number of factors in Eq. (14). Provided that the sum over γ is dominated by sufficiently few terms and that the factors can be viewed as statistically independent, $\ln \Delta$ becomes normally distributed by the central limit theorem. The small deviations of the splitting distribution for $dh = 0$ from a log-normal distribution, as shown in Fig. 1(c), indicate the degree to which these assumptions are justified. In particular, one may expect that for larger values of Δ , the sum in Eq. (14) is dominated by rare terms, which take on a large value. In contrast, more trajectories contribute to the splitting for smaller values of Δ , leading to deviations from a log-normal distribution in the small- Δ tail. Moreover, the splittings Δ have an upper cutoff given by the many-body level spacing, leading to deviations in the large- Δ tail.

The two degenerate ground states of the transverse field Ising model in the limit of zero transverse field contain no domain walls. Thus, their splitting is due to tunneling processes with intermediate states of excitation energy $\sim J$ and, consequently, in the limit under consideration, much smaller than the splitting of excited states.

We remark that the assumption of $J \ll 1$ was made to simplify the presentation. None of our results depend on it in essential ways. In fact, we can use a stroboscopic Floquet perturbation theory [27] (see also Sec. III C) to discuss the eigenphases for general J , with the same qualitative results.

B. Fermionized model

For zero random longitudinal field ($dh = 0$), the Floquet Ising model is integrable, and its many-body spectrum is composed of single-particle levels. We can investigate the distribution of π pairings from the viewpoint of these single-particle levels.

A Jordan-Wigner transformation maps the Floquet quantum Ising model to a free-fermion model in two ways (see the Appendix) [21,22]. If we apply the Jordan-Wigner transformation to the original spin operators, the fermion operators c_j effectively describe spin flips in the transverse field basis, and the Floquet operator takes the form

$$U_{F,0} = P \exp \left\{ \frac{i\pi\delta g}{2} \sum_{j=1}^N (1 - 2c_j^\dagger c_j) \right\} \times \exp \left\{ \frac{i\pi}{2} \sum_{j=1}^N J_j (c_j^\dagger c_{j+1} - c_j^\dagger c_{j+1}^\dagger) + \text{H.c.} \right\}. \quad (15)$$

Here, we identify $c_{N+1} = -Pc_1$. Thus, while the original spin model has periodic boundary conditions, the fermionized model has periodic (antiperiodic) boundary conditions for $P = -1$ ($P = 1$). This difference between the Neveu-Schwarz ($P = -1$) and Ramond ($P = 1$) sectors of the model appears since the Jordan-Wigner string in $Z_N Z_1$ winds around the

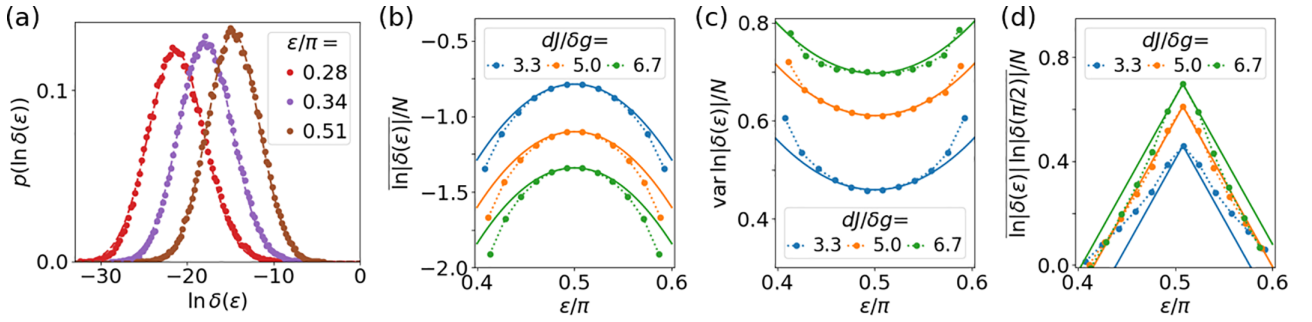


FIG. 3. Single-particle splittings $\delta(\epsilon)$ for different boundary conditions of the Jordan-Wigner fermions and various energies ϵ in the band. (a) Distributions across the disorder ensemble (dots). Dashed lines: log-normal fits. (b) Average, (c) variance, and (d) correlations of $\ln|\delta(\epsilon)|$ (dotted lines). Solid lines show the perturbation theory. Lines have been shifted by a constant. Parameters are as follows: $J = 0.5$ and $\mathcal{N} = 10^5$ disorder realizations in all plots; $dJ = 0.25$, $N = 18$, and $g = 0.9$ in (a); and $dJ = 0.1$ and $N = 12$ in (b)–(d) (for g see legends).

entire chain. In the fermionic representation, the spin-flip symmetry maps P to the fermion parity $P = \prod_j e^{i\pi c_j^\dagger c_j}$.

In the limit of small δg , it is advantageous to apply the Jordan-Wigner transformation to the dual spin operators describing domain walls. The corresponding fermion operators

$$d_j^\dagger = \frac{1}{2}(c_j + c_j^\dagger + c_{j+1} - c_{j+1}^\dagger) \quad (16)$$

effectively describe domain walls. In terms of these operators, the Floquet operator takes the form

$$U_{F,0} = P \exp \left\{ \frac{i\pi\delta g}{2} \sum_{j=1}^N (d_j + d_j^\dagger)(d_{j-1} - d_{j-1}^\dagger) \right\} \times \exp \left\{ \frac{i\pi}{2} \sum_{j=1}^N J_j (1 - 2d_j^\dagger d_j) \right\}. \quad (17)$$

Analogous to the convention for the spin-flip fermions c_j , the domain-wall fermions satisfy $d_0 = -Pd_N$ (see the Appendix). Due to the noninteracting nature of this fermion problem, the eigenphases of $U_{F,0}$ can be written as $E[\{n_\alpha\}] = \sum_\alpha n_\alpha \epsilon_\alpha$, where n_j are fermionic occupation numbers and ϵ_α are single-particle eigenphases.

In the limit defined in Eq. (12), we can combine the exponentials, so that apart from the factor P , $U_{F,0}$ reduces to the time-evolution operator of

$$H = \frac{\pi\delta g}{2} \sum_{j=1}^N (d_j + d_j^\dagger)(d_{j-1}^\dagger - d_{j-1}) + \pi \sum_{j=1}^N J_j d_j^\dagger d_j. \quad (18)$$

The contributions of the pairing terms (corresponding to the generation or annihilation of pairs of domain walls) are parametrically suppressed in a perturbative expansion in δg , so that the Hamiltonian reduces to a noninteracting Anderson model with random on-site disorder. Moreover, we already saw in Sec. III A that, to leading order, we can neglect the dependence of the ground-state energy on P . Thus, the splittings of the π pairs arise from the dependence of the single-particle excitations on P .

The Anderson models for $P = \pm 1$ effectively differ by a π flux threading the ring or, equivalently, in their boundary conditions. As argued by Thouless [28], the sensitivity of the

single-particle levels to the boundary conditions is a measure of the conductance of the system. Moreover, the conductance of a one-dimensional disordered wire obeys a log-normal distribution [23] as a consequence of Oseledec's theorem [29]. We thus conclude that the single-particle splittings $\delta_\alpha = \epsilon_\alpha(P = +1) - \epsilon_\alpha(P = -1)$ have a log-normal distribution. This expectation is in excellent agreement with the numerical data in Fig. 3(a).

These conclusions can be understood as follows. As a consequence of Anderson localization, the corresponding difference in the single-particle energies is exponentially small in $N/\xi(\epsilon)$, where $\xi(\epsilon)$ is the localization length at the energy ϵ of the single-particle excitation. In zeroth order in the transverse field, the single-particle spectrum consists of fermions localized at sites j with energy πJ_j , so that $\epsilon/\pi \in [J - dJ, J + dJ]$. A nonzero transverse field introduces hopping between nearest-neighbor sites. The splitting between the $P = \pm 1$ sectors is due to hopping around the entire chain, which appears in N th-order perturbation theory. Thus, the splitting of the excitation with $\epsilon = \pi J_j$ is given by the amplitude

$$\delta_j \simeq 2\pi\delta g \prod_{l(\neq j)} \frac{\pi\delta g/2}{\epsilon - \pi J_l}. \quad (19)$$

This expression is a limiting case of an exact relation with a similar structure [30].

Unlike in the perturbative approach to the many-body eigenphases E_n in Sec. III A, only two terms of equal amplitude contribute to Eq. (19) at this order of perturbation theory, and the factors are statistically independent. The log-normal distribution is thus a direct consequence of the central limit theorem. As for the many-body eigenphases, we can characterize the splitting distribution of the single-particle eigenphases by

$$\overline{\ln \delta(\epsilon)} = -\frac{N}{\xi(\epsilon)}, \quad \text{var} \ln \delta(\epsilon) = \frac{N}{\ell(\epsilon)} \quad (20)$$

in terms of the localization length $\xi(\epsilon)$ and the elastic mean free path $\ell(\epsilon)$ of the Anderson model [31]. Using Eq. (19) for $N \gg 1$ and small $\epsilon - \pi J$, we find

$$\overline{\ln |\delta(\epsilon)|} \simeq -N \left[\ln \frac{2dJ}{e\delta g} + \frac{(\epsilon - \pi J)^2}{2(\pi dJ)^2} \right] \quad (21)$$

and

$$\text{var} \ln |\delta(\epsilon)| \simeq N \left[1 + \frac{(\epsilon - \pi J)^2}{(\pi dJ)^2} \right]. \quad (22)$$

The expression for $\overline{\ln |\delta(\epsilon)|}$ shows that states near the band edges are most strongly localized. Correspondingly, their splitting fluctuations $\text{var} \ln |\delta(\epsilon)|$ are largest. The dependence of these quantities on ϵ is in good agreement with numerical results within the range of validity of the expansion in $\epsilon - \pi J$ [see Figs. 3(b) and 3(c)]. We remark that the limit defined in Eq. (12) is challenging to realize numerically. Deviations necessitate an additional overall vertical shift of the fitting curves in Figs. 3(b) and 3(c). Consistent with expectations, the shift diminishes when approaching the limit in Eq. (12).

The splitting Δ of many-body eigenphases is given as a sum of many log-normally distributed single-particle splittings δ . Since a log-normal distribution has a finite average and variance, one may be tempted to apply the central limit theorem and conclude that Δ should have a normal distribution, in contradiction to the observed log-normal distribution. This conundrum is resolved by noting that the single-particle splittings violate the assumption of statistical independence underlying the central limit theorem. In fact, the single-particle splittings are correlated even for states with widely differing energies. We can use Eq. (19) to compute the (connected) correlations of the single-particle splittings at different energies. Working to first order in $\epsilon - \epsilon'$, we find

$$\overline{(\ln |\delta(\epsilon)| \ln |\delta(\epsilon')|)^{(c)}} \simeq N \left[1 - \frac{|\epsilon - \epsilon'| \ln^2(\pi dJ)}{2\pi dJ} \right]. \quad (23)$$

This result is in good agreement with numerical results, as shown in Fig. 3(d), and explains the kink at $\epsilon = \epsilon'$. The correlations drop on a scale $\epsilon_c = \frac{2\pi dJ}{\ln^2(\pi dJ)}$, so that the single-particle splittings are correlated over a wide range of energies. This precludes the application of the central limit theorem to the sum over single-particle splittings and explains how the log-normal distribution of the many-body splittings emerges from the log-normally distributed single-particle splittings.

C. Random longitudinal field

We now turn to a discussion of the random longitudinal field, which breaks integrability as well as the global spin-flip symmetry P . As shown in Fig. 1(a), the log-normal splitting distribution persists in the presence of a random longitudinal field. We find that the mean grows with the strength of the longitudinal field, while the width in $\ln \Delta$ shrinks (with a corresponding increase in peak height). As shown in Fig. 2, the mean and the width of the distribution in $\ln \Delta$ continue to depend exponentially on chain length N , with the length scales $\xi(dh)$ and $\ell(dh)$ in Eq. (5) increasing with field.

The effect of the random longitudinal field can be understood within a stroboscopic Floquet perturbation theory for $U_F = U_{F,0} e^{iV}$, where we treat $V = \sum_j h_j Z_j$ as a perturbation [27]. Expanding the eigenphases $E_n = E_{n,0} + E_{n,1} + E_{n,2} +$

\dots of U_F to quadratic order in V gives

$$E_{n,1} = \langle n_0 | V | n_0 \rangle \quad (24)$$

and

$$E_{n,2} = \sum_{m \neq n} \frac{|\langle n_0 | V | m_0 \rangle|^2}{2 \tan \frac{E_{n,0} - E_{m,0}}{2}}. \quad (25)$$

Here, the unperturbed eigenstates $|n_0\rangle$ of $U_{F,0}$ are assumed to be nondegenerate with eigenphases $E_{n,0}$. We denote the unperturbed π pairs as $|n_0, \pm\rangle$ with $P|n_0, \pm\rangle = \pm|n_0, \pm\rangle$ and unperturbed many-body splittings as

$$\Delta_{n_0} = \pi - E_{n_0}^+ + E_{n_0}^-. \quad (26)$$

The longitudinal field is odd under P , so it couples states with opposite parities. As a result, the first-order contribution vanishes, and Eq. (25) gives the perturbed splittings

$$\Delta_n \simeq \Delta_{n_0} - \sum_m \left[\frac{|v_{nm}^{+-}|^2}{2 \tan \frac{E_{n,+} - E_{m,-}}{2}} - \frac{|v_{nm}^{+}|^2}{2 \tan \frac{E_{n,-} - E_{m,+}}{2}} \right], \quad (27)$$

with matrix elements $v_{nm}^{+-} = \langle n, + | V | m, - \rangle$.

In Eq. (27), we have made the perturbation theory self-consistent by inserting the exact eigenphases into the denominators [27]. This is motivated as follows. While the divergent eigenphase denominator suppresses the contribution of π pairs (i.e., the terms with $m = n$), there are many terms of similar magnitude with $m \neq n$. This is plausibly captured by a self-consistent approximation. An analogous scheme was applied successfully to the related problem of Majorana π modes in chains with open boundary conditions [27].

We make the splittings $\Delta_n = \pi - E_n^+ + E_n^-$ explicit in the energy denominators and expand in them as they are small compared to the eigenphase differences. To linear order, we find

$$\Delta_n \simeq \Delta_{n,0} + \Lambda_n - \Sigma_n \Delta_n \quad (28)$$

in terms of

$$\Lambda_n \simeq \sum_m \left[\frac{|v_{nm}^{+-}|^2}{2 \tan \frac{E_{n,0}^+ - E_{m,0}^+ + \pi}{2}} - \frac{|v_{nm}^{+}|^2}{2 \tan \frac{E_{n,0}^- - E_{m,0}^+ + \pi}{2}} \right], \quad (29)$$

$$\Sigma_n \simeq \sum_m \left[\frac{|v_{nm}^{+-}|^2}{4 \cos^2 \frac{E_{n,0}^- - E_{m,0}^-}{2}} + \frac{|v_{nm}^{+}|^2}{4 \cos^2 \frac{E_{n,0}^+ - E_{m,0}^+}{2}} \right]. \quad (30)$$

In defining Σ_n and Λ_n , we assume that the exact eigenphases E_n^\pm can now be replaced by their unperturbed counterparts $E_{n,0}^\pm$. Solving for Δ_n , we find

$$\Delta_n \simeq \frac{\Delta_{n,0} + \Lambda_n}{1 + \Sigma_n}, \quad (31)$$

similar to an analogous expression in Ref. [27].

Figure 4 shows that the splitting distributions in the presence of random longitudinal field are well reproduced by the self-consistent perturbation theory. Deviations from the log-normal fits appear deep in the tails of the distribution, as shown in the inset.

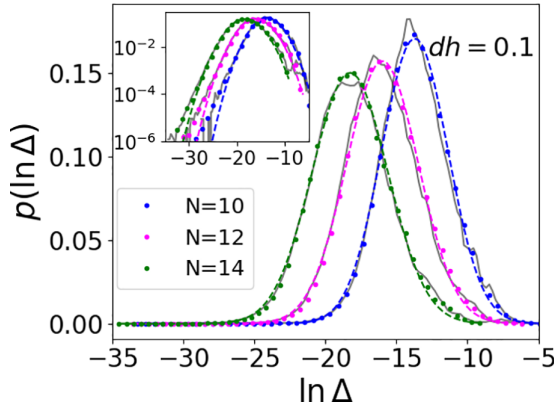


FIG. 4. Distribution of the many-body splittings with disordered longitudinal field for various chain lengths (see legend). Numerical data (symbols) are compared to the self-consistent perturbation theory (solid gray lines). Dashed line: log-normal fits to data. Inset: Same as in the main plot, but on a doubly logarithmic scale. Parameters are $J = 0.5$, $dJ = 0.25$, $g = 0.95$, $\mathcal{N} = 10^4$ disorder realizations for $N = 10, 12$, and $\mathcal{N} = 2 \times 10^3$ disorder realizations for $N = 14$.

IV. CONCLUSION

Floquet time crystals with a subharmonic response at half the driving frequency are known to exhibit π pairing in their eigenphase spectrum [13,14]. In finite-size systems, the eigenphase difference splits away from π by an exponentially small amount. We showed that the probability distribution of these splittings across the many-body spectrum and the disorder ensemble is well approximated by a log-normal distribution. Moreover, its Fourier transform is directly proportional to the temporal spin correlations of finite-size time crystals. This provides an immediate relation between the spectral statistics of the Floquet operator and the defining characteristic of Floquet time crystals.

Our results open various avenues for further research. First, it is an interesting question whether other spin correlation functions can be related to the spectral statistics of π pairings. In particular, recent work emphasized the role of out-of-time-order correlators of Floquet time crystals [32]. Second, it is important to understand whether a similar relation between spectral statistics and time-crystalline order extends to Floquet time crystals with other subharmonic periods [14,33–35], to time-crystalline behavior in open quantum systems [36–41], or to disorder-free models [42–44]. Third, our work relies on a combination of numerical simulations and analytical arguments. It would be interesting to see whether the relation between spin correlations and splitting distributions as well as the latter’s log-normal nature can be made rigorous.

Our results may also have implications for the phase diagram of Floquet time crystals. It is natural to speculate that the relation between the pairing distribution and time-crystalline spin correlations is a basic property of the time-crystal phase. This would suggest that the time-crystal phase requires the spectral π pairing to be well-defined, i.e., that the splittings are small compared to the many-body level spacing of order 2^{-N} . Under these assumptions, the condition in Eq. (8) for the existence of well-defined splittings describes the phase boundary of the time-crystal phase. It would thus be interest-

ing to understand the dependence of the characteristic length ζ on system parameters. This line of thinking may also have ramifications for the existence of time crystals in more than one dimension.

ACKNOWLEDGMENTS

We thank R. Fazio, S. Sondhi, and K. Yang for helpful discussions. We gratefully acknowledge funding from Deutsche Forschungsgemeinschaft through CRC 183, as well as the Einstein Research Unit on Quantum Devices (FvO), and from NSF Grant No. DMR-2410182 (L.I.G.). We thank the HPC service of ZEDAT, Freie Universität Berlin, for computing time [45].

DATA AVAILABILITY

The data that support the findings of this article are openly available [46].

APPENDIX: JORDAN-WIGNER TRANSFORMATION

We use the Jordan-Wigner transformation

$$X_j = 1 - 2c_j^\dagger c_j; \quad Z_j = i(c_j^\dagger - c_j) \exp \left\{ i\pi \sum_{l < j} c_l^\dagger c_l \right\}. \quad (\text{A1})$$

This implies

$$Y_j = -iZ_j X_j = (c_j + c_j^\dagger) \exp \left\{ i\pi \sum_{l < j} c_l^\dagger c_l \right\}, \quad (\text{A2})$$

so that the spin raising and lowering operators $S_j^\pm = \frac{1}{2}(Y_j \pm iZ_j)$ become

$$S_j^+ = c_j e^{i\pi \sum_{l < j} c_l^\dagger c_l}, \quad S_j^- = c_j^\dagger e^{i\pi \sum_{l < j} c_l^\dagger c_l}. \quad (\text{A3})$$

We associate c_j^\dagger with the spin-lowering operator S_j^- because the latter creates a spin-flip excitation in the paramagnetic phase.

We introduce Majorana operators defined by

$$c_j = \frac{1}{2}(a_j + ib_j), \quad (\text{A4})$$

so that

$$X_j = -ia_j b_j, \quad Y_j = a_j \prod_{l < j} (-ia_l b_l), \quad Z_j = b_j \prod_{l < j} (-ia_l b_l).$$

We can express the Floquet quantum Ising model with periodic boundary conditions in terms of the Majorana operators using

$$g \sum_{j=1}^N X_j = -ig \sum_{j=1}^N a_j b_j \quad (\text{A5})$$

and

$$\sum_{j=1}^N J_j Z_j Z_{j+1} = i \sum_{j=1}^N J_j a_j b_{j+1}. \quad (\text{A6})$$

We note that $Z_N Z_1 = -iP a_N b_1$, which we accounted for by the conventions $c_{N+1} = -P c_1$, $a_{N+1} = -P a_1$, and $b_{N+1} = -P b_1$.

Note that in these conventions, $P = \pm 1$ denotes the sector of Hilbert space and is no longer an operator.

In terms of the spin-flip operators c_j , we have

$$g \sum_{j=1}^N X_j = g \sum_{j=1}^N (1 - 2c_j^\dagger c_j) \quad (\text{A7})$$

and

$$\sum_{j=1}^N J_j Z_j Z_{j+1} = \sum_{j=1}^N J_j (c_j + c_j^\dagger)(c_{j+1} - c_{j+1}^\dagger). \quad (\text{A8})$$

In this formulation, spin flips cost a Zeeman energy of $2g$, while the exchange coupling either hops the spin flip to a neighboring site or creates or annihilates a pair of spin flips on nearest-neighbor sites.

We can also define fermions for which the exchange term becomes diagonal,

$$d_j^\dagger = \frac{1}{2}(a_j + ib_{j+1}). \quad (\text{A9})$$

They are associated with the dual representation of the quantum Ising model in terms of domain-wall operators. In fact, $d_j^\dagger d_j$ counts the number of domain walls at the bond between sites j and $j + 1$,

$$\sum_{j=1}^N J_j Z_j Z_{j+1} = \sum_{j=1}^N J_j (1 - 2d_j^\dagger d_j). \quad (\text{A10})$$

Moreover, the transverse field term turns into

$$g \sum_{j=1}^N X_j = g \sum_{j=1}^N (d_j + d_j^\dagger)(d_{j-1} - d_{j-1}^\dagger). \quad (\text{A11})$$

In this formulation, domain walls cost an exchange energy of $2J$, while the Zeeman coupling either hops the domain walls to a neighboring bond or creates or annihilates a pair of domain walls on nearest-neighbor bonds.

We finally discuss the influence of the fermion parity P on the domain-wall representation. Recalling the sign convention for the fermion operators, we note that

$$d_N^\dagger = \frac{1}{2}(a_N + ib_{N+1}) = \frac{1}{2}(a_N - ib_1 P), \quad (\text{A12})$$

so that

$$iJ_N a_N b_{N+1} = -iJ_N P a_N b_1 = J_N (1 - 2d_N^\dagger d_N) \quad (\text{A13})$$

and

$$-iga_1 b_1 = gP(d_1 + d_1^\dagger)(d_N^\dagger - d_N). \quad (\text{A14})$$

This is consistent with Eqs. (A10) and (A11) if we use the convention $d_0 = -Pd_N$.

-
- [1] F. Wilczek, Quantum time crystals, *Phys. Rev. Lett.* **109**, 160401 (2012).
- [2] K. Sacha and J. Zakrzewski, Time crystals: A review, *Rep. Prog. Phys.* **81**, 016401 (2018).
- [3] V. Khemani, R. Moessner, and S. L. Sondhi, A brief history of time crystals, [arXiv:1910.10745](https://arxiv.org/abs/1910.10745).
- [4] S. Choi, Observation of discrete time-crystalline order in a disordered dipolar many-body system, *Nature (London)* **543**, 221 (2017).
- [5] J. Zhang, Observation of a discrete time crystal, *Nature (London)* **543**, 217 (2017).
- [6] J. Randall, C. E. Bradley, F. V. van der Gronden, A. Galicia, M. H. Abobeih, M. Markham, D. J. Twitchen, F. Machado, N. Y. Yao, and T. H. Taminiau, Many-body-localized discrete time crystal with a programmable spin-based quantum simulator, *Science* **374**, 1474 (2021).
- [7] X. Mi, Time-crystalline eigenstate order on a quantum processor, *Nature (London)* **601**, 531 (2022).
- [8] P. Frey and S. Rachel, Realization of a discrete time crystal on 57 qubits of a quantum computer, *Sci. Adv.* **8**, eabm7652 (2022).
- [9] D. V. Else, C. Monroe, C. Nayak, and N. Y. Yao, Discrete time crystals, *Annu. Rev. Condens. Matter Phys.* **11**, 467 (2020).
- [10] M. P. Zaletel, M. Lukin, C. Monroe, C. Nayak, F. Wilczek, and N. Y. Yao, *Colloquium: Quantum and classical discrete time crystals*, *Rev. Mod. Phys.* **95**, 031001 (2023).
- [11] V. Khemani, A. Lazarides, R. Moessner, and S. L. Sondhi, Phase structure of driven quantum systems, *Phys. Rev. Lett.* **116**, 250401 (2016).
- [12] D. V. Else, B. Bauer, and C. Nayak, Floquet time crystals, *Phys. Rev. Lett.* **117**, 090402 (2016).
- [13] C. W. von Keyserlingk, V. Khemani, and S. L. Sondhi, Absolute stability and spatiotemporal long-range order in Floquet systems, *Phys. Rev. B* **94**, 085112 (2016).
- [14] F. M. Surace, A. Russomanno, M. Dalmonte, A. Silva, R. Fazio, and F. Iemini, Floquet time crystals in clock models, *Phys. Rev. B* **99**, 104303 (2019).
- [15] A. Lazarides, A. Das, and R. Moessner, Fate of many-body localization under periodic driving, *Phys. Rev. Lett.* **115**, 030402 (2015).
- [16] N. Y. Yao, A. C. Potter, I.-D. Potirniche, and A. Vishwanath, Discrete time crystals: Rigidity, criticality, and realizations, *Phys. Rev. Lett.* **118**, 030401 (2017).
- [17] P. Ponte, Z. Papić, F. Huveneers, and D. A. Abanin, Many-body localization in periodically driven systems, *Phys. Rev. Lett.* **114**, 140401 (2015).
- [18] E. Bairey, G. Refael, and N. H. Lindner, Driving induced many-body localization, *Phys. Rev. B* **96**, 020201(R) (2017).
- [19] M. Sonner, M. Serbyn, Z. Papić, and D. A. Abanin, Thouless energy across the many-body localization transition in Floquet systems, *Phys. Rev. B* **104**, L081112 (2021).
- [20] P. Sierant, M. Lewenstein, A. Scardicchio, and J. Zakrzewski, Stability of many-body localization in Floquet systems, *Phys. Rev. B* **107**, 115132 (2023).
- [21] E. Lieb, T. Schultz, and D. Mattis, Two soluble models of an antiferromagnetic chain, *Ann. Phys. (NY)* **16**, 407 (1961).
- [22] P. Pfeuty, An exact result for the 1D random Ising model in a transverse field, *Phys. Lett. A* **72**, 245 (1979).
- [23] Y. Imry, Active transmission channels and universal conductance fluctuations, *Europhys. Lett.* **1**, 249 (1986).

- [24] M. Titov, D. Braun, and Y. V. Fyodorov, Log-normal distribution of level curvatures in the localized regime: Analytical verification, *J. Phys. A* **30**, L339 (1997).
- [25] P. W. Brouwer, M. Duckheim, A. Romito, and F. von Oppen, Probability distribution of Majorana end-state energies in disordered wires, *Phys. Rev. Lett.* **107**, 196804 (2011).
- [26] S. Asmussen, J. L. Jensen, and L. Rojas-Nandayapa, On the Laplace transform of the lognormal distribution, *Methodol. Comput. Appl. Probab.* **18**, 441 (2016).
- [27] H. Schmid, A.-G. Penner, K. Yang, L. Glazman, and F. von Oppen, Robust spectral π pairing in the random-field Floquet quantum Ising model, *Phys. Rev. Lett.* **132**, 210401 (2024).
- [28] D. J. Thouless, Maximum metallic resistance in thin wires, *Phys. Rev. Lett.* **39**, 1167 (1977).
- [29] V. I. Oseledec, A multiplicative ergodic theorem, Lyapunov characteristic numbers for dynamical systems, *Trans. Moscow Math. Soc.* **19**, 197 (1968).
- [30] D. J. Thouless, A relation between the density of states and range of localization for one dimensional random systems, *J. Phys. C* **5**, 77 (1972).
- [31] D. J. Thouless, Percolation and localization, in *Ill-Condensed Matter*, edited by R. Balian, R. Maynard, and G. Toulouse, Ecole d'ete de Physique Theoretique Les Houches (North-Holland, Amsterdam, 1979), p. 1.
- [32] H. Sahu and F. Iemini, Information scrambling and entanglement dynamics in Floquet time crystals, *Phys. Rev. B* **111**, 104302 (2025).
- [33] A. Pizzi, J. Knolle, and A. Nunnenkamp, Period- n discrete time crystals and quasicrystals with ultracold bosons, *Phys. Rev. Lett.* **123**, 150601 (2019).
- [34] A. Pizzi, J. Knolle, and A. Nunnenkamp, Higher-order and fractional discrete time crystals in clean long-range interacting systems, *Nat. Commun.* **12**, 2341 (2021).
- [35] G. Giachetti, A. Solfanelli, L. Correale, and N. Defenu, Fractal nature of high-order time crystal phases, *Phys. Rev. B* **108**, L140102 (2023).
- [36] F. Iemini, A. Russomanno, J. Keeling, M. Schirò, M. Dalmonte, and R. Fazio, Boundary time crystals, *Phys. Rev. Lett.* **121**, 035301 (2018).
- [37] K. Tucker, B. Zhu, R. J. Lewis-Swan, J. Marino, F. Jimenez, J. G. Restrepo, and A. M. Rey, Shattered time: Can a dissipative time crystal survive many-body correlations? *New J. Phys.* **20**, 123003 (2018).
- [38] B. Zhu, J. Marino, N. Y. Yao, M. D. Lukin, and E. A. Demler, Dicke time crystals in driven-dissipative quantum many-body systems, *New J. Phys.* **21**, 073028 (2019).
- [39] F. M. Gambetta, F. Carollo, M. Marcuzzi, J. P. Garrahan, and I. Lesanovsky, Discrete time crystals in the absence of manifest symmetries or disorder in open quantum systems, *Phys. Rev. Lett.* **122**, 015701 (2019).
- [40] C. Booker, B. Bua, and D. Jaksch, Non-stationarity and dissipative time crystals: Spectral properties and finite-size effects, *New J. Phys.* **22**, 085007 (2020).
- [41] M. Krishna, P. Solanki, M. Hajdušek, and S. Vinjanampathy, Measurement-induced continuous time crystals, *Phys. Rev. Lett.* **130**, 150401 (2023).
- [42] E. van Nieuwenburg, Y. Baum, and G. Refael, From Bloch oscillations to many-body localization in clean interacting systems, *Proc. Natl. Acad. Sci. USA* **116**, 9269 (2019).
- [43] A. Kshetrimayum, J. Eisert, and D. M. Kennes, Stark time crystals: Symmetry breaking in space and time, *Phys. Rev. B* **102**, 195116 (2020).
- [44] S. Liu, S.-X. Zhang, C.-Y. Hsieh, S. Zhang, and H. Yao, Discrete time crystal enabled by stark many-body localization, *Phys. Rev. Lett.* **130**, 120403 (2023).
- [45] L. Bennett, B. Melchers, and B. Proppe, Curta: A General-purpose High-Performance Computer at ZEDAT, Freie Universität Berlin (2020).
- [46] A.-G. Penner, H. Schmid, L. Glazman, and F. von Oppen, Data and plotting scripts for "Subharmonic spin correlations and spectral pairing in Floquet time crystals," Zenodo, 2025, <https://doi.org/10.5281/zenodo.15270135>